

Modeling transport in stellarator island divertors in the presence of magnetic chaos

S. O. Makarov^{1,2}, F. Reimold¹, N. Maaziz¹, R. Davies¹, E. Rodríguez¹, and V. R. Winters¹
and W7-X team

¹ Max-Planck-Institut für Plasmaphysik, Wendelsteinstraße 1, 17491 Greifswald, Germany

² Max-Planck-Institut für Plasmaphysik, Boltzmannstraße 2, 85748 Garching, Germany

Corresponding author mail: sergei.o.makarov@gmail.com

The island divertor is a promising exhaust concept for future stellarator reactors [1], based on magnetic islands formed by resonant perturbations. In practice, real coil spectra and MHD effects can trigger additional resonances, creating magnetic field chaos (MFC). While chaos in Hamiltonian systems and fusion-relevant fields has been widely studied [2], prior work often focuses on large domains where chaos acts diffusively [3]. In contrast, MFC in island divertors typically involves a single dominant resonance intersecting solid structures, limiting chaotic mixing. As a result, plasma properties can align with localized structures such as turnstile lobes [4], channeling heat to remote target areas [5] and potentially damaging plasma-facing components.

We present a Hamiltonian model to study magnetic field chaos in island divertors, where island chains form atop circular flux surfaces. Its flexibility allows for comprehensive exploration of perturbation spectra and target geometries, extending MFC studies beyond the limitations of fixed-coil setups. The model generates field-aligned grids for EMC3-EIRENE using 2D meshing and field-line tracing.

The magnetic field takes the general form:

$$2\pi\mathbf{B} = \nabla\psi \times \nabla\theta + \nabla\phi \times \nabla\chi$$

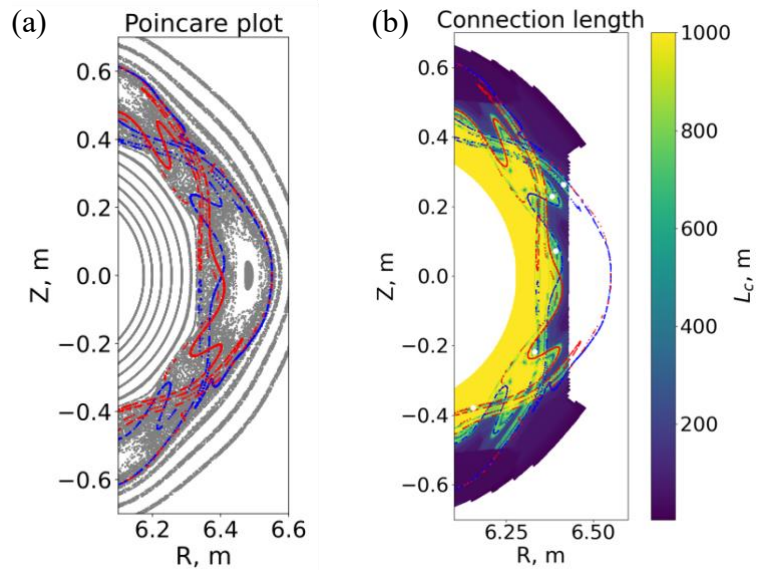


Figure 1. Poincaré plot (a) and connection length plot (b) at $\phi = 0^\circ$ in the case with magnetic field chaos (MFC). Red dots represent manifolds traced in the forward direction, and blue dots represent manifolds traced in the backward direction. White circles indicate areas attributed to a common turnstile lobe

The field line trajectory is governed by a Hamiltonian system:

$$\frac{d\psi}{d\phi} = -\frac{\partial\chi}{\partial\theta}, \quad \frac{d\theta}{d\phi} = \frac{\partial\chi}{\partial\psi} \quad (1)$$

Here, the poloidal magnetic flux is:

$$\chi(\psi, \theta, \phi) = \chi_0(\psi) + \sum_{\alpha=1}^{n_{\text{pert}}} \chi_{\alpha}(\psi) \cos[m_{\alpha}(\theta - \iota_{\alpha}^{\text{res}}\phi)]$$

Here, $\chi_{\alpha}(\psi) = A_{\alpha}f_{\alpha}(\psi)$ where $f_{\alpha}=1$ at the reference ψ . In the large aspect ratio limit, assuming the toroidal magnetic field scales as $\sim 1/R$, where R is a major radius, one can derive the relation between canonical (ψ, θ, ϕ) and elementary toroidal (r, ϑ, φ) coordinates:

$$\psi = \pi r^2 B_0 \quad \theta = \vartheta - \varepsilon \sin \vartheta, \quad \phi = \varphi$$

We chose the $\psi(r)$ dependence to construct flux surfaces with circular cross-sections. Here, $B_0=1\text{T}$. A linear iota profile is chosen to locally match a W7-X-like iota profile:

$$\iota(\psi) = d\chi_0/d\psi = a_{\iota}\psi + b_{\iota}$$

The primary perturbation ($n_1=5, m_1=5, A_1=-6\times 10^{-4}\text{Wb}, B_1\approx 1.4\times 10^{-4}\text{T}$) generates the main island chain intersected by the discontinuous target [1]. In the absence of additional perturbations (no chaos case), flux surfaces are preserved within the island, the core, and the private flux region (PFR).

The secondary perturbation ($n_2=10, m_2=11, A_2=-2.4\times 10^{-4}\text{Wb}, B_2\approx 1.3\times 10^{-4}\text{T}$) induces magnetic field chaos (MFC) within the island divertor.

The Hamiltonian system (1) is solved using fourth-order symplectic Yoshida integrator [6] to trace field lines, construct the Poincaré plot (Figure 1a), and compute manifolds and connection lengths (Figure 1b).

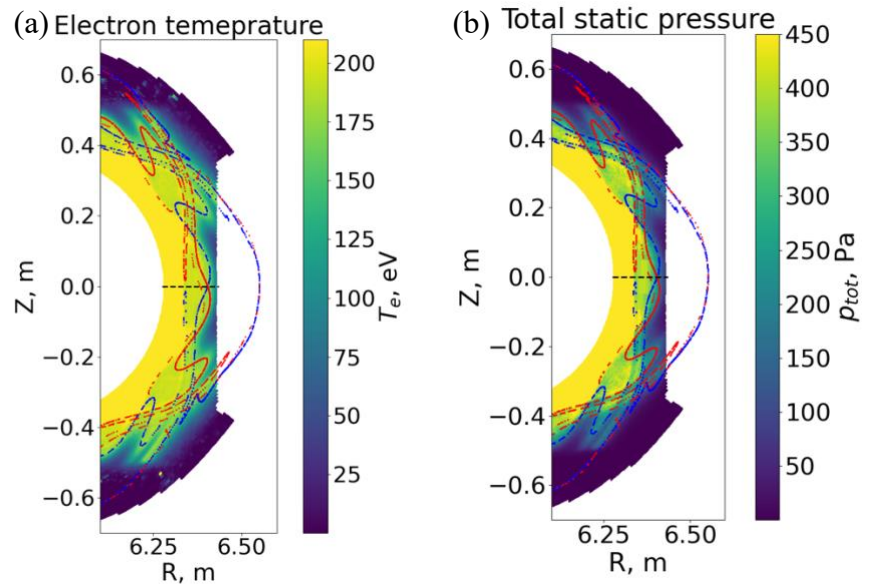


Figure 2. 2D electron temperature distribution (a) and 2D total static pressure distribution (b) at $\varphi = 0^\circ$ in the case with magnetic field chaos (MFC). Red dots represent manifolds traced in the forward direction, and blue dots represent manifolds traced in the backward direction. The dashed black line marks the location of radial (midplane) profile

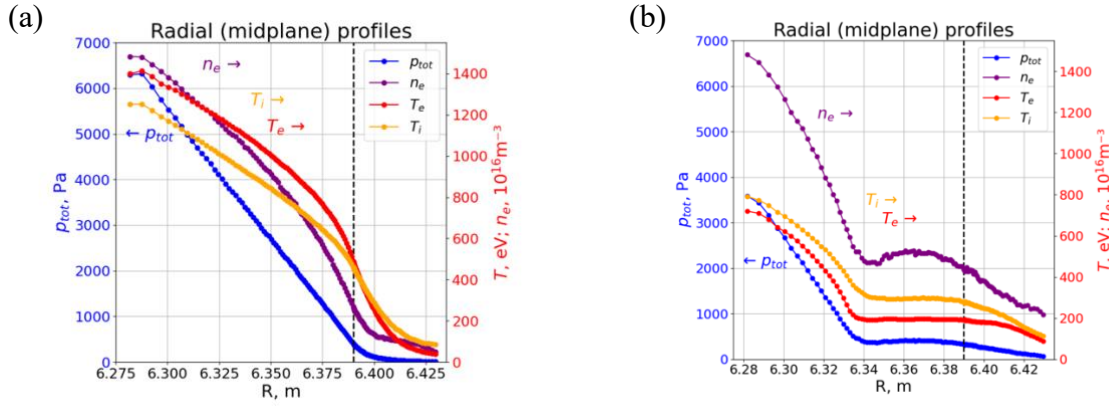


Figure 3. Profiles of density, electron and ion temperatures, and total static pressure at the outer midplane ($Z = 0$, $\varphi = 0^\circ$; dashed line in figure 2) in the cases without (a) and with (b) magnetic field chaos (MFC). The vertical dashed line indicates the separatrix position in the no-MFC case.

The manifolds constrain the region of intact flux surfaces (Figure 1a). Heat from the core is captured by turnstile lobes and efficiently transported through the chaotic region to the target (white circles in Figure 1b) after only a few mappings.

An EMC3-EIRENE grid was also generated using our field-line tracing procedure. We simulated transport for both the no-chaos and MFC cases, prescribing electron and ion heat fluxes, electron density at the core boundary, and anomalous transport coefficients

$$\chi_{e,i}^{anom} = 1.5m^2/s \quad \text{and} \quad D_i^{anom} = 0.2m^2/s \quad .$$

Figure 2 shows that both T_e and p_{tot} are nearly uniform within the turnstile regions, as cross-field anomalous transport efficiently equalizes them across neighboring field lines. Thus, heat transport is largely driven by the dynamics of the turnstile lobes.

In the no-chaos case (Figure 3a), steep gradients develop at the island separatrix due to anomalous diffusion. In contrast, the MFC case (Figure 3b) shows flattened profiles across the chaotic region, with sharp gradients confined to the remaining closed-flux surfaces.

The presence of chaos reduces the effective confinement volume and degrades core performance: $p_{tot}^{core} = 3600$ Pa in the MFC case vs. 6300 Pa without MFC.

As shown in Figure 4, the secondary strike line and heat deposition between turnstile lobes enhance heat spreading on the target beyond the effect of anomalous transport alone, reducing the peak heat flux by approximately 20%. This may aid heat exhaust management in future stellarator reactors, depending on how accurately the model captures experimental conditions.

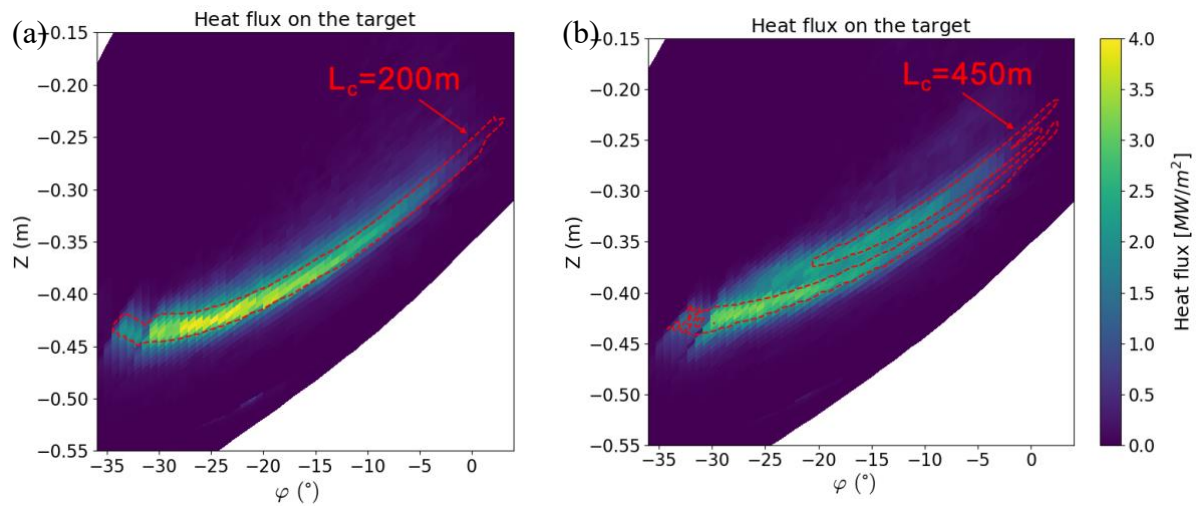


Figure 4. Heat flux deposition on the right part of the target in the cases without (a) and with (b) magnetic field chaos (MFC). The red dashed contour indicates the region of long connection length.

Conclusions

- A Hamiltonian model was developed for EMC3-EIRENE grid generation and to study magnetic field chaos in island divertor configurations.
- Unlike stochastic diffusion [3], the chaos induces localized transport structures—such as turnstiles [4,5]—which govern heat flow.
- Heat is channeled along turnstile-lobe structures, efficiently transporting energy from nested flux surfaces through the chaotic layer to the divertor target.
- Despite its strong effect on core plasma profiles, magnetic field chaos has a surprisingly limited impact on target parameters.
- The peak heat flux is reduced by $\sim 20\%$, offering potential benefits for power exhaust in stellarator reactors.
- However, the associated confinement degradation may outweigh this benefit.

References

- [1] Y. Feng and W7-X-team, Plasma Physics and Controlled Fusion 64, 125012 (2022).
- [2] P. Helander, S. R. Hudson, and E. J. Paul, Journal of Plasma Physics 88, 905880122 (2022).
- [3] A. B. Rechester and M. N. Rosenbluth, Phys. Rev. Lett. 40, 38 (1978).
- [4] J. D. Meiss, Chaos: An Interdisciplinary Journal of Nonlinear Science 25, 097602 (2015)
- [5] A. Punjabi and A. H. Boozer, Physics of Plasmas 29, 012502 (2022).
- [6] H. Yoshida, Physics Letters A 150, 262 (1990)